

VISUAL EVENT RELATED POTENTIALS. THE ORIGIN OF WAVE P300. A COMPUTER MODEL*

O. FEHÉR** and R. SCHNELL***

Department of Comparative Physiology,
University of Szeged, Közép fasor 52, H-6726 Szeged, Hungary

(Received: June 5, 2002; accepted: July 1, 2002)

This five-layered model consisting of 180 neurons is aimed at simulating some elementary functions of primary visual cortex of mammals in form detection.

Its main achievements are:

1. Detection of points, lines, simple geometric figures in the V1
2. Abstraction of 19 different qualities of geometric figures
3. Simulation and rational explanation of processing of peripheral stimuli in the V1, explanation of mechanism of origin of visual ERPs, including P300 wave
4. Simulation and explanation of the nature and build up of the cognitive function within V1 and its possible relation to long-term memory
5. The model is based partly on Hebb-type synapses, illustrates the role of *neuronal assemblies*, sheds light on the functional relationship of excitatory and inhibitory neurons, in their conformity with special tasks of different cortical layers.

Keywords: Visual cortex, event related potentials, P300, computer model

INTRODUCTION

Analytical neurosciences have attained deep insight into structure and functioning of the nervous system. Sophisticated methods of ultrastructure research, histochemistry, immuno-chemistry, biochemical analysis, nucleic acid chemistry, analysis of gene activation and its products, research of early steps of ontogenesis, of neural regeneration, use of transgenic animals are yielding an amazing, never seen picture of the living material and especially of the nervous system. Among other bio-sciences, nerve physiology made enormous progress in the second half of the 20th century. Membrane processes, analysed mainly by bio-physicists and electrophysiologists has reached the most fundamental steps of bio-electric phenomena by recording activity of single ionic channels and cloning them together with transmitter receptors acti-

* Dedicated to Professor György Ádám on the occasion of his 80th birthday.

** Corresponding author

*** Present address: Department of Microbiology, S-10691 Stockholm, Sweden

ating them. On the other hand, methods giving overall pictures of activity of extensive brain areas or even of the whole brain, like EEG, PET, SPECT or magnetic methods help pursuing detection of dynamics, localizations, intensity changes of brain functions allowing to discover correlations between objectively recorded physiological events and subjective sensations, thoughts and motivations of waking humans.

However, a tremendous gap is extending between the pictures given by analytical methods on one hand, and those painted by the group of holistic approaches on the other. None of them is able to answer the question: how is functioning the brain as a system, what kinds of neural processes underlie to consciousness, motivations, emotions, logical thinking, memory, moral judgements, phantasy and human creativity. Although most part of these psychic and mental capacities can be regarded as subjects of psychology, one never can elude the question, what are their physiological, bio-cybernetical equivalents in the brain and in which way can they be analysed, given the methodology of neuro- and psychobiology of to day. At the moment no research paradigms exist, which could describe the functioning of a neural sub-system beginning with single neurons up to the system's structure, yielding an integrated explanation of its achievements and motives of behaviour. Learning the connectivity plan, localizing the sites and special roles of each neuron and building up above the morphological structure a detailed functional, one can attain the total comprehension.

Since no methodology is able to execute this sequence of steps, neurobiology is in need of some special kinds of procedures to circumvent the tremendous gap between analytical and holistic methods of investigation. A conceptual way to fill this gap is proposed by modeling nervous structures and systems. The immense body of literature shows, that the usefulness of this way has widely been recognized not only by neurobiologists but by a lot of peoples of quite different professions: mathematicians, physicists, chemists, engineers and scientists engaged in quite different branches of biology. The basic paradigm of modeling neuronal substrates is, that well-known analytical data are to be arranged in systems, which have analogous structure with those of the nerves or more complex neural organs and try to let them operate and look at the result: is it similar or comparable with that of the modeled neural substrate. If any analogy with the modeled neural structure is recognized, one can draw conclusions as to its inner connectivity, mode of operation, physiological role and location in the whole system. This may give ideas for future research and satisfy the need for causality of the model-maker. Modeling is therefore not a by-product but an indispensable tool of neurobiological research.

The network character of the nervous system determines the basic principles of modeling. The bricks of the model, the neurons must be endowed with all the capacities necessary for building up a network. Other special features have to be integrated into this main one. This requirement may be exemplified with the Internet: the elements of this net, the single computers must owe all of the input-output circuits indispensable for participation in it, but many other special features remain irrelevant. This parsimony saves a lot of memory and time.

Further questions are: 1. which functions of the neuron must be included in the model neuron and 2. how other details of structure and function become integrated into the main profile.

Method of modeling

The *model neuron* (further on *neuron*) is an input-output device, being able to integrate the impinging stimuli and thus becomes also in itself a source of impulses. Its basic state variable is the membrane potential held at rest at an arbitrary value 48. Stimulating (depolarizing) impulses elevate it, while inhibitory hyperpolarizing impulses act contrarily. The overall level of polarization is made up by linear summation of the two kinds of polarization changes.

An important value of this state variable is *threshold*, at which the neuron becomes enabled to fire, i.e. send out action potentials (spikes). The threshold is at different neuron types between 51 and 60. The spike frequencies may vary from 1 to 9, depending on the momentary level of depolarization. The spikes reach all of the axonal endings. The excursions of the membrane potential from both directions decay exponentially to the resting value with definite time constants, and needs (when undisturbed) 7 cycles (see Appendix).

The model is operated from the keyboard. At first the number and configuration of the stimuli is set, then the number of cycles to be run. Each stimulus paradigm can be repeated at will. One cycle of the system is taken as equivalent with 8–10 ms in the living system. Each spike increases the depolarization of the postsynaptic cell at a definite rate (see Appendix). If the postsynaptic neuron is at the time of arrival of the spike in depolarized state, the synapse becomes strengthened according to the *Hebb-rule* and governed by a function detailed in the Appendix. As mentioned above, neurons are excitatory or inhibitory in character, but differ from one another in some other respects, too.

Synapses

In the neurons no soma-axon-dendrite fractionation was defined. Excitatory impulses are received on 21 synaptic ports in each neuron. Excitatory actions impinging upon different synaptic ports become summated linearly. If a synaptic port was facilitated previously, shows higher synaptic strength, mentioning that a spike will elevate the local depolarization stronger than on non-facilitated ones. Since no axon has been defined, excitatory and inhibitory influences are represented by appropriate program steps. Inhibitory impulses impinge on one synaptic port on each neuron, but they influence the overall membrane potential. Conduction times on axons or dendrites have not been defined as well, because postsynaptic potentials evoked by them are of incomparably longer duration.

As mentioned earlier, if an excitatory ending encounters a neuron in excited state, his postsynaptic port will be facilitated at a rate, depending on the frequency (see Appendix). However, this state is not constant but subject to further influences: it may be enhanced by further excitatory stimuli or, during rest, it decays at a low rate. Hebbian synapses are connecting and concatenating groups of neurons activated by a stimulus paradigm; they were named by Hebb *neuronal assemblies*, serving as functional units of the cortical network. On the other side, synaptic endings, which are not able to activate their postsynaptic targets or cannot participate in their activation, are gradually weakening.

The model network

The network is built up by five layers, denoted with letters B, C, D, E and F. In layer B are housed 20 excitatory neurons, the other four consist of 20 excitatory and 20 inhibitory cells. On the whole the model is built up by 180 neurons. The input layer is B, but also layer E and F can be activated immediately for special purposes from the keyboard. Beginning with layer B the rest of the structure is sequentially activated in the order B-C-D-E-F, but feedback connections in relation of E-D and F-E reverse the direction of the impulse flow (Fig. 1). The neurons of layer B are regarded as members of a quadratic matrix consisting of 4×4 neurons while four cells are situated beyond it at the middle of the four sides (Fig. 2.) They are cortical repre-

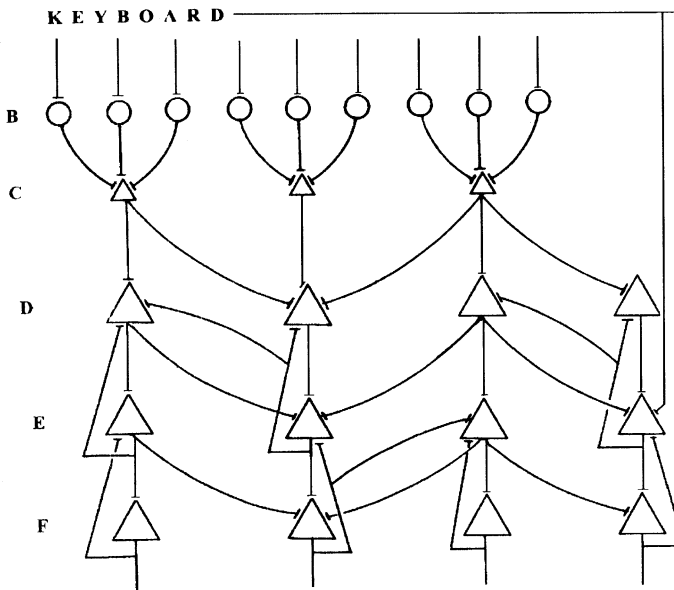


Fig. 1. Connectivity plan of 9 excitatory neurons of layer B. Inhibitory neurons are not illustrated

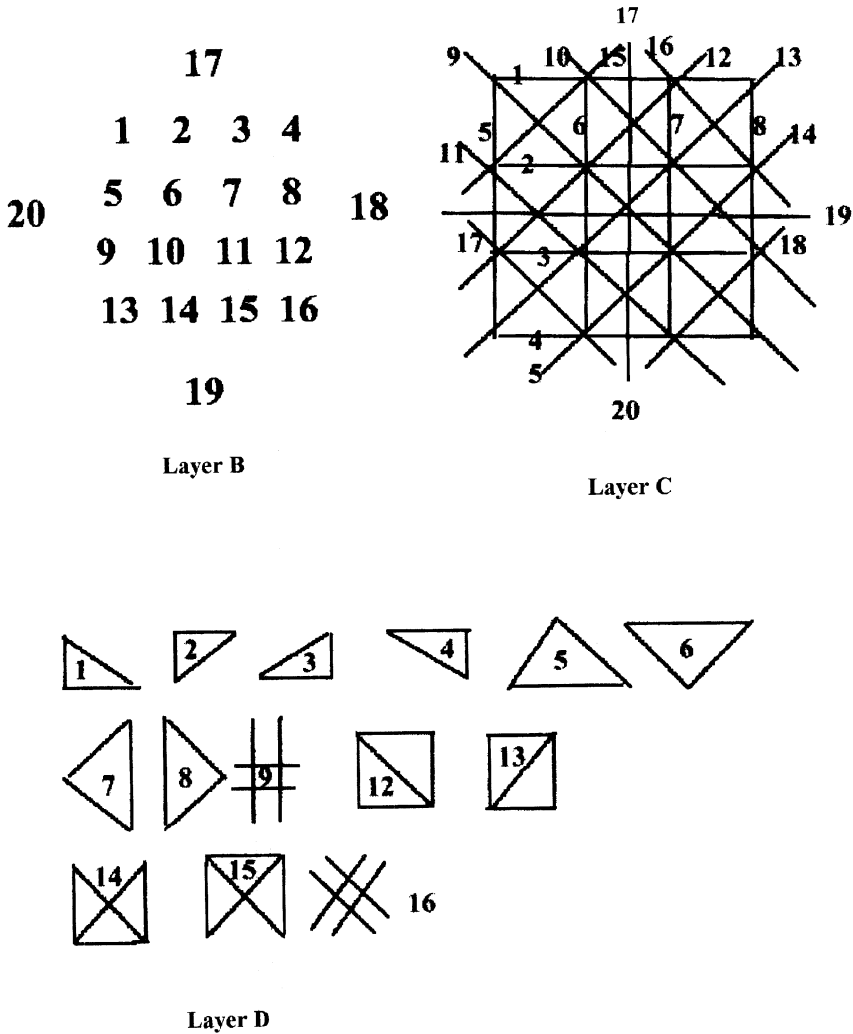


Fig. 2. Top left: The quadratic array of layer B neurons, which correspond to 20 photoreceptors of the *Macula lutea* of the retina. Top right: Lines denote neurons of layer C, which represent 20 linear stimuli falling in four different directions on the retina. Bottom: Geometric figures composed from lines of layer C, synthesised and represented by neurons of layer D and numbered from 1 to 16. They will be quoted as D1 to D16 in the following

representatives of type P ganglion cells in the fovea centralis of the retina. Straight lines connecting points of this matrix converge on single neurons of layer C and form a system of orientation selective neurons in number 20. Those lines of layer C, which define simple geometric figures converge on neurons of layer D. In this 18 neurons represent triangles squares, crosses and other geometric figures which are activated

only if corresponding stimulus configuration arises from layer B. Members of layer D possessing identical structural details converge on definite neurons of layer E. Thus geometric figures, which are “triangular”, square-shaped or contain cross, excite convergently the appropriate neurons, expressing the abstracted qualities “close”, “open”, “top”, “bottom” etc. are represented by neurons of layer E. The function of layer F will be discussed later (Fig. 3).

1 small	2 large	3 closed	4 open
triangle		square	
5 cross	6 column	7 left r.a.	8 right r.a.
9 bottom r.a.	10 top r.a.	11 oblique	12 diagonal
13 double diagonal	14 top open	15 bottom open	
16 top traverse	17 bottom tr.	18 standing left	19 standing right

large triangle

r.a. denotes the position of the right angle of the triangle

Fig. 3. Abstracted qualities of geometric figures of layer D and represented by neurons of layer E. r.a. denotes the position of the right angle of the triangle

The neural structure modeled

According to previous studies M type ganglion cells subservise mainly movement sensing and their central projections are restricted mainly to the cytochrom-oxydase rich blobs of the cortex. Their visual field is quite large. The smaller P type neurons have smaller visual fields and are represented in the “inter-blob” stripes of the cortex. They are engaged in the shape detection. Central representation of K type ganglion cells awaits clarification.

Our model is centered on the central representation of the P type ganglion cells, all the more, because this has been most successfully investigated and most part of physiological data has been derived from them [6, 7] Fig. 4. Depicts the main intracortical connections of their thalamo-cortical afferents, the cells activated by them in different layers of the cortex. Letters written in the neurons denote layers of the model corresponding to them in Fig. 4. According to this, layer B corresponds to the interneurons of cortical layer 4C β , which are excited by the LGB afferents. Their

“visual field” is circular so they lack any orientation or directional selectivity. The numerical and topographical relation to retinal P ganglion cells is one to one. Ascending axons of B-cells innervate neurons of layer C (corresponding to cortical layer 4A.) so, that B-cells excited by a straight line converge on the same C-neuron and this gains in this way orientation selectivity. Combinations of 20 B-neurons make up 20 lines represented by the same number of C-neurons exhibiting orientation selectivity over 360 degrees at every 45 degrees (see Fig. 2). The selectivity of orientation specificity needs focusing, because every B-neuron participating in build-up of a given line “is used” also by four lines differing by 25–175 degrees of orientation selectivity. Therefore excitation of a B-neuron belonging to one line will excite all the neurons of lines dissecting it, in subthreshold manner. This requires a system of inhibitory neurons, which depress the excitation of the dissecting and even the parallel lines, helping to give emphasis to the really stimulated one. In this way the acti-

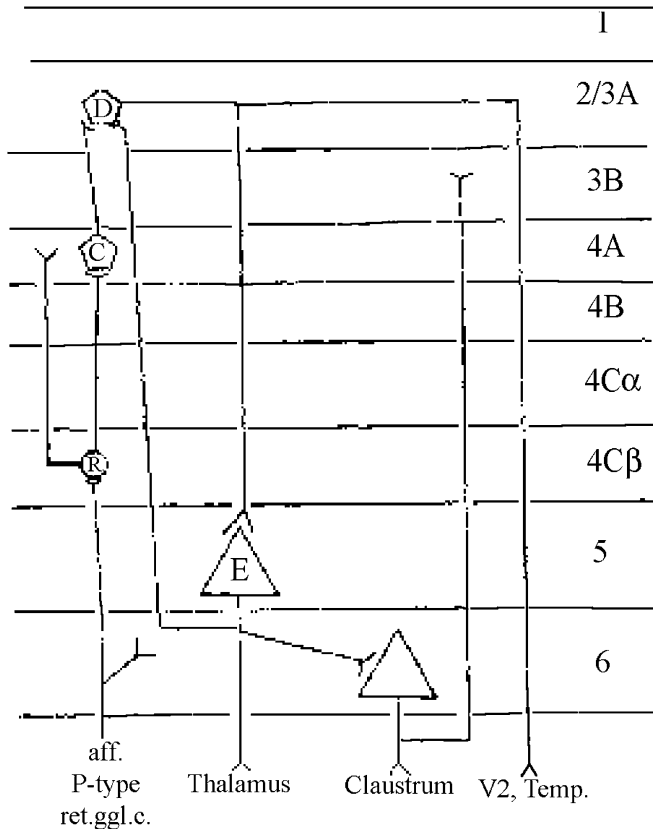


Fig. 4. Neuronal network of central representation of P type ganglion cells in V1 cortex of *Macaca nemertina*, as described by Callaway (1). Letters written in the neurons refer to their theoretical positions in the model

vated neurons, safely held by inhibitory cells, become competent, sharply distinguished from the momentarily not used or even inhibited ones.

The next synaptic connection leads excitation from layer 4A to layer 2/3A in which neurons presumably represent simple geometric figures synthesized by lines of layer 4A. In the model this step is carried out by axons innervating neurons of layer D. This layer yields 16 geometric figures, represented by D-series of neurons (Fig. 2). Introduction of inhibitory neurons was also here necessary between similar and diagonally dissimilar figures, respectively.

Neurons including similar details converge to selected neurons of layer E. Nineteen E-layer neurons substantiate primary abstraction of the geometric figures. In real cortical network this function may be localized in the large pyramidal cells of layer 5 or in the V2 (Fig. 3). A feedback pathway connects cells of layer E to cells of layer D in such a way that the formers excite D-cells immediately activating them. This may also be a model of *recall* by layer E and all the other cortical structures sending fibers to it. In normal functioning of the visual cortex this reverberatory circuit may help fixation of traces of excitation in the long-term memory.

Layer F is activated by layer E but quite otherwise, than it was usual between former layers. The innervation coming from layer E is organized in random manner. The

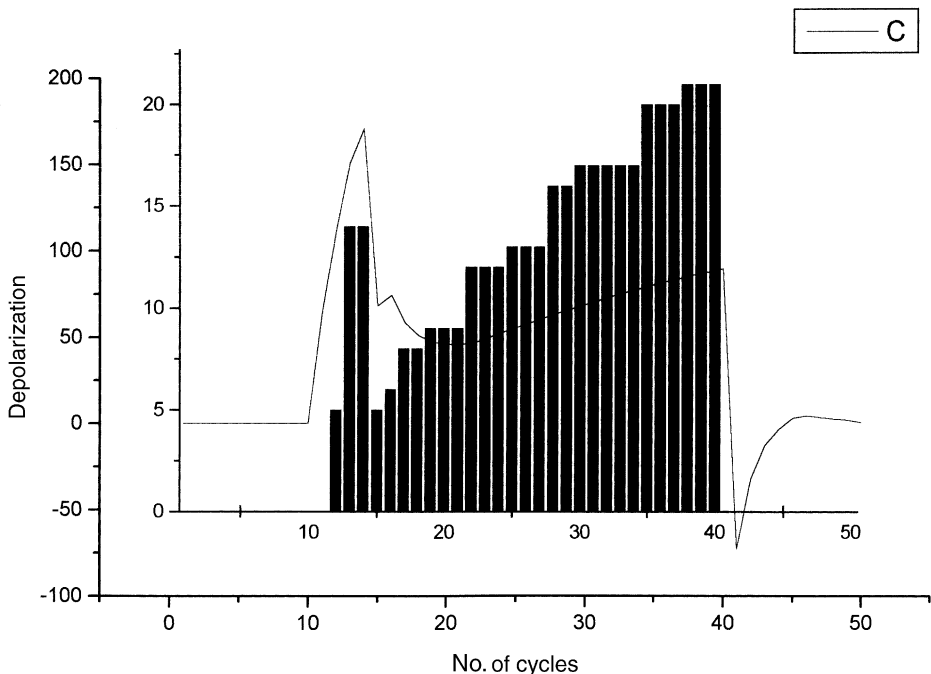


Fig. 5. Field potentials (line, outer coordinate system) and spike discharges (columns, inner coordinate system) of layer C neurons during presentation of triangle D1 throughout 30 cycles. Ordinate of the inner coordinate system is scaled as Spikes/cycle

ramification of each E axon reaches 5 F-neurons but without any topographical or logical order. Each F-neuron is connected to an inhibitory cell, which send axons to each F-cells with exception of the one, activating them. Each F-neuron sends feedback axons to E-cells innervating them. This is assumed to be analogous with mode of operation of the right hemisphere and apt to record time sequences of input pulses. The exact site of this type of cortical structures was not defined thus far, maybe it is housed in the right hemisphere or even in the V3 of the same side.

The feedback connection to layer E does not lead to irradiation of excitation or to chaotic circulation of excitation in reverberating circuits; on the contrary it helps the selection of competent neurons (usually 2–4 cells) bound specifically to the actual situation in layer E. Recall by direct activation of layer F is possible, but not as exactly as from layer E.

RESULTS

The dynamics of impulse propagation in the cortex

In accordance with the cortical structure, the source of the thalamocortical fibers is the LGB, layer B in the model, whose neurons innervate 3 neurons in layer C on somato-topical grounds. Stimulation of a given row of cones by linear pattern, activates rows of B-neurons which, in turn, converge on a specific cell in layer C, an equivalent of cortical layer 4A in the brain. Thus layer C neurons are endowed with orientation selectivity. Since one B-neuron projects to 3 C-neurons 3 B-neurons throw 9 C neurons into activity or subthreshold excitation. To keep orientation selectivity, this initial irradiation becomes controlled by a system of inhibitory cells and after several cycles a group of competent neurons remains only active. The rest of the layer sinks into hyperpolarization or remains in resting state. This sequence of events is shown in Fig. 5 in the field potential record of layer C. In case of the D12 square (with one diagonal) five lines represent the competent neurons (for 4 sides and the diagonal) the rest is inactive or inhibited. After the first 10 cycles the depolarization of the layer goes on to elevate until the end of the stimulation as a consequence of synaptic facilitation. This extends, of course, only to competent neurons.

The cellular activity (rows of columns in Fig. 5) roughly duplicates the course of the field potential. It begins with 5/cycle jumps for 2 cycles (3 B-neurons times 3) then falls back to 5/cycle (in cycle 15) due to inhibition coming from the five neurons which are going to be competent. Afterwards it begins to rise and attains 20/cycle value in eight steps until the end of stimulation. This is the apparent manifestation of the Hebb-type facilitation built in this type of synapse: synaptic efficacy rises from 1 to 4 spikes/cycle.

Layer D, the first cognitive structure, recognizes the geometric patterns defined by the lines of layer C, starts activity with irradiation of excitation, as well. The field potential curve (Fig. 6) shows a pike of about 80 units, then an even sharper pike of hyperpolarization down to -270 and then rises again to $+70$. This is followed by a

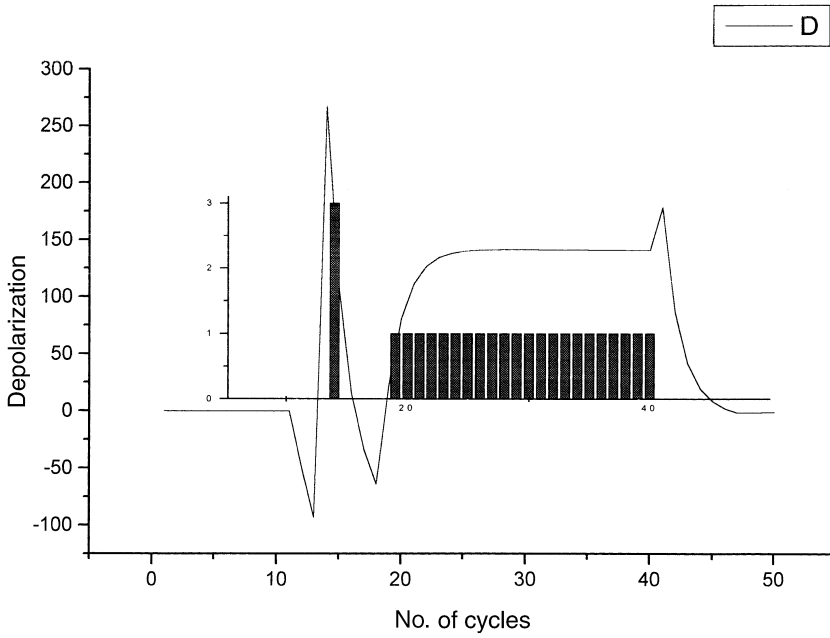


Fig. 6. Field potentials and spike discharges of layer D under the same conditions as in layer C

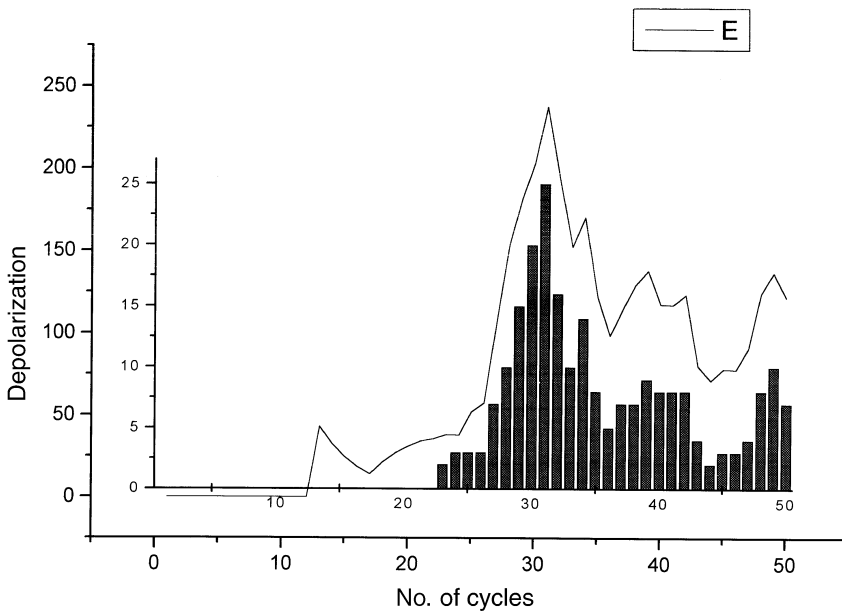


Fig. 7. Field potentials and spike discharges of layer E under the same conditions as in layer C

sink to -150 and remains there until end of stimulation. This is an apparent sign of a steady and strong inhibition dominating the whole layer decaying in 7 cycles with the end of stimulus.

The cellular record allows a deeper insight into the sequence of events. The column attaining 4 spikes/cycle reflects the activation of four D-neurons: one of them is D12, the main target of bombardment, two of them represent triangles D1 and D4 included in square D12, and finally appears D15, an open square with two diagonals. The entrance of inhibition activated by D12 redraws the overall picture: beginning with cycle 23 all the neurons, with exception to D12, fall in deep inhibition: the selection of the only competent neuron, D12 has been fulfilled. This is the firm basis of recognition.

The factual activity of layer E commences at cycle 23, as impulses from layer D have arrived (Fig. 7). Layer E evaluates four qualities of the D12 square: its size, shape, the existence and starting point of the diagonal. The four impulses informing about the mentioned qualities evoke an initial depolarization up to $+230$, then it relaxes and keeps between $+40$ and 130 . This stems from the special structure of inhibition in layer E. Neurons representing adverse qualities (small-large, left right, triangle-square, etc., see Table E) inhibit each other. This helps the selection of the competent neurons giving the abstraction of the figurine recognized by layer D. At the same time they give opportunity to store it in memory and prepare retrieval. The easiest way to realize all this is to send impulses of competent E-cells into reverberating circuits and give opportunity to fixate them in facilitated synapses.

Therefore layer E-cells innervate neurons of the fifth layer of the model, of layer F consisting of 20 principal and 20 inhibitory neurons as well in such a way that every E-neuron activates 5 F-cells selected in random manner (Fig. 8). The axon of each F-cell innervates in feedback mode that very E-neuron which activates it. Thus an inter-layer reverberation is built up after each package of stimulus, which is able to store its traces in form of facilitated synapses and hold them also throughout periods of silence. This arrangement may give some example for the role of cortical rhythms in maintaining and consolidating memory traces in the brain.

Another conditionally used feed-back loop is built in from layer E or F to layer D which serves modeling of retrieval of memory traces stored in the E-F circuit in form of synaptic facilitation. In our opinion layer E and F may serve as interface from and to the abstract-logical apparatus of the brain and visual memory.

Morphology of the visual event related potentials (VERPs). The origin of the P300 wave

A macroelectrode placed on the cortical surface picks up voltage changes of the brain. Since cortical tissue acts as a low-pass-filter, only low-frequency potential changes (up to 80 Hz) are transmitted to the electrode. Steeply rising, fast potential waves (like spike discharges of single neurons) remain beyond the scope of this kind of recording, therefore electrocorticographic and electroencephalographic records

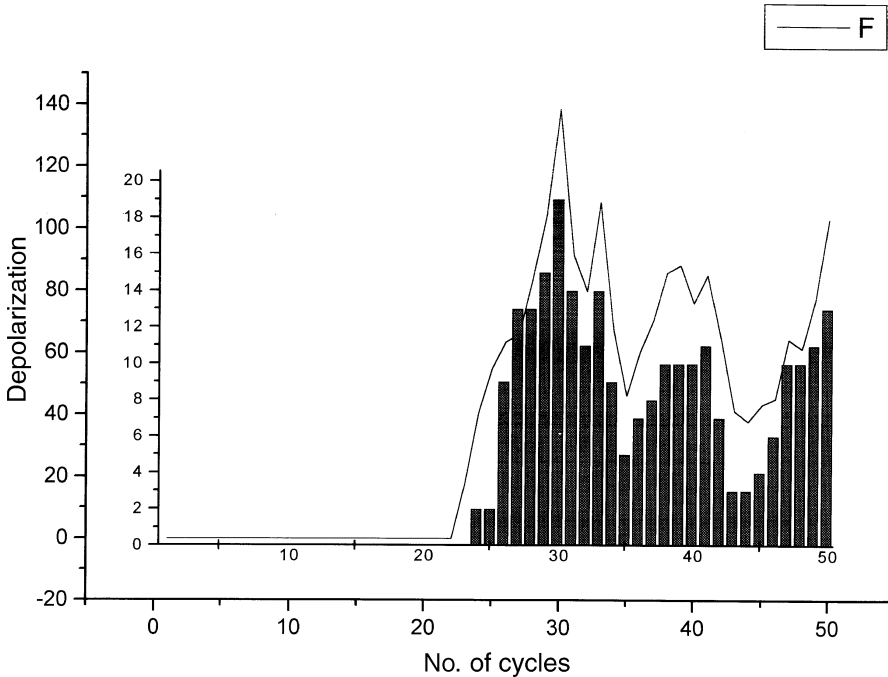


Fig. 8. Field potentials and spike discharges of layer F under the same conditions as in layer C

give a rather one-sided picture about brain function. The slow potentials take their origin from local synaptic potentials and other slowly moving waves of high inertia and take place mainly in the somato-dendritic membrane of the neurons and in the glial cells. At local depolarization of a cell slow sodium- and calcium current enters the membrane but in remote regions other positive-mainly potassium-ions leave and make these places positive. In this way cells become dipoles, being polarized at their length. If a good number of such cells are vertically oriented to the cortical surface, their synchronous depolarization may create considerable potential differences between cortical surface and deeper layers or among even cortical layers. These slowly moving large masses of charged particles lead to electrographic phenomena and gross electrodes record them as *field potentials*. Under the cover of these overall potential changes a tremendous stream of vivid, high frequency bursts of neurons is rumbling and at present no physiological method is able to give an integrated picture of these two kinds of manifestations of central neural function. At this step is entering *computer modelling*, which, using experimental experience is able to build up schemes of neural nets and make observations on relations of systemic and singular-cellular functions in order to explore how systemic action is integrated from single cell's activities and adversely: what electrographic records tell us about actual function.

Most important components of neural circuits in the cortex are vertically oriented and represent dipoles. So, deeply situated local depolarizations appear on the surface as positive waves and inhibitions give negative deflections. At neurons near to the surface correspond electric waves to their original nature. In case of intermingled and interactive currents of four-five different subsets of neurons only detailed deep-electrode measurements, multi-layer electrode techniques give reliable picture. In computer simulation this experience is used and gives opportunity to extrapolate from small subsets of neurons to functionally more comprehensive systems like visual cortex.

In the present model as derived from the hodological data [1] C-layer (4A layer) neurons start vertically (normally) to the cortical surface and EPSPs of their cell somata and dendrites will be reflected as positive waves on the surface. Layer D neurons (histological layer 2/3 A) take place practically on the surface and therefore their potential changes appear in their original polarity in the surface electrogram. Layer E and F neurons (cells of the 5 and 6 histological layer) are again in the depth, also vertically oriented, and so inversely represented at the surface electrode. In constructing the electrogram of the model VERP the above assumptions were used so, that field potential curves of the C-D-E-F layers, seen in Figures 5–8 were averaged, with exception for layer D, with inversed polarity (Fig. 9) and the result of this procedure is shown in Figure 10, in case of D1 small triangle. Transition zones of the different potentials as inflection points are denoted together with portions representing the sequence of appearance of the layers' field potentials. For comparison an experimentally recorded VERP from human scalp (by Antal A. and coll., 1998, lower record) is shown in Figure 11. Besides the basic likelihood, two obvious differences between the experimental and model picture must be emphasized: the experimental record begins with a small negative peak, while the model pattern has in this place a positive wavelet. The small initial negativity is usually explained as the depolarization wave of the thalamocortical endings. In the model this detail is not included and therefore not illustrated. A major difference is observable in the shape of the first positive wave at about 220 ms latency of the scalp record. Instead, in the model curve a rather sharp positive peak is present. This is the sign of the strong inhibitory accident which prepares the d3 depolarization i.e. the selection of the competent neuron in layer D. This selection requires a rather strong inhibitory intervention in order to get rid of D4 triangle, D12 and D15 squares, discharging during the initial excitatory irradiation and all this must be done in three cycles. Maybe, under natural circumstances all this takes longer time and the first positive wave is much broader. D1 triangle is probably represented by more than one neuron and also the number of inhibitory neurons is much more than the one charged at this aim in the model. The third cognitive layer, layer F for sake of clarity has been omitted. However oscillations between layers E and F left traces on field potential E and in the scalp record similar oscillations in this portion of the curve are abundant. We assume that there exists some structure in the brain engaged in processing informations coming from layer E near to or even within the visual cortex. In any case, it is remarkable, that best P300 waves could be led off from the scalp in derivations with Cz-mastoid-electrode

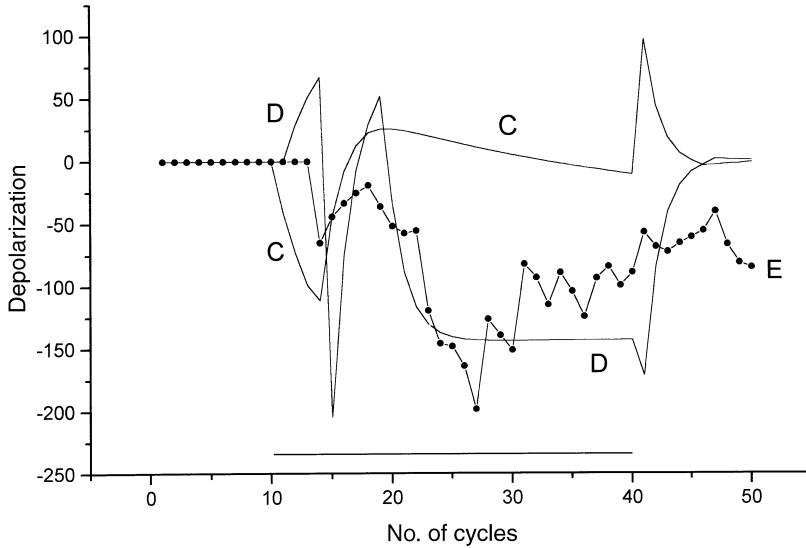


Fig. 9. Composite picture of field potentials of layers C, D, E, during presentation of triangle D1. (For sake of clarity, curve of layer F has been omitted.) Bias of layers C and E is inverted according to their localisation in the cortical depth

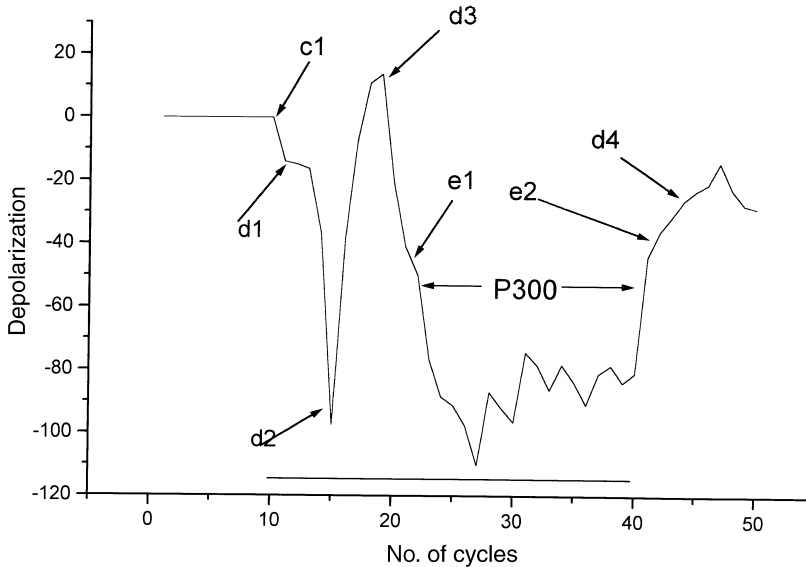


Fig. 10. Summated picture of field potentials derived from layers C, D and E as it can be recorded by a macroelectrode from the cortical surface or from the scalp. Letters denote inflection points, indicating transitions between field potentials of different layers. The presumed position of the wave P300 is indicated. Other waves of the experimental VERP (see Fig. 11), recognizable in the model curve, are: P100 at d2, N150 at d3, and P300 between e1 and e2. N140 of the experimental curve is lacking

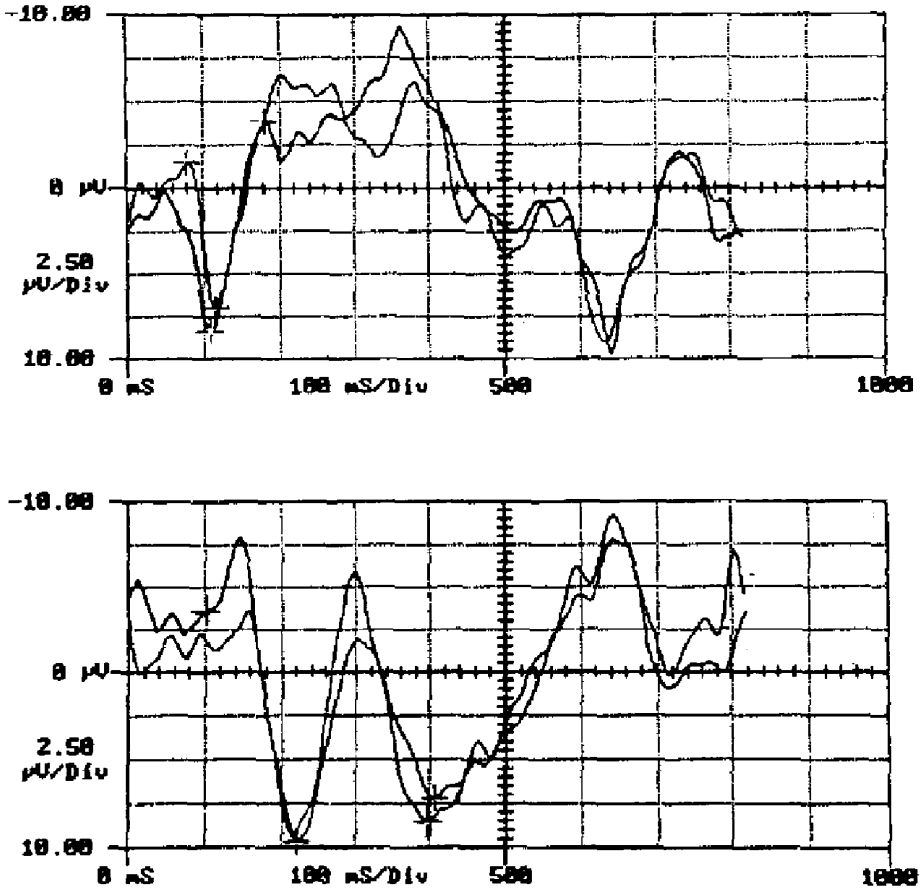


Fig. 11. Averaged primary (Oz, F1) and cognitive (Cz, mastoid) visual event related potentials from human scalp at stimulation of the right eye. Positivity downward [Antal et al., 10]

pair [9], which embraces the whole occipital lobe, with visual centers and visuomotor pathways included.

In building up P300 basically two potential components participate: the inhibitory phase of the D pattern and the initial depolarization phase of layer E. The transition of wave D to wave E is observable as a fine inflection point at e1 in the model curve and in numerous EEG records taken from humans and monkeys. The two components separate themselves at e2 in the model and another inflection point in the EEG records (not illustrated here) when rates of repolarization of the two waves begin to differ.

Although depolarization of layer E commences at the 13 cycle, it becomes dominant from cycles 23 until end of stimulus, in this case cycle 40. At repeated stimuli,

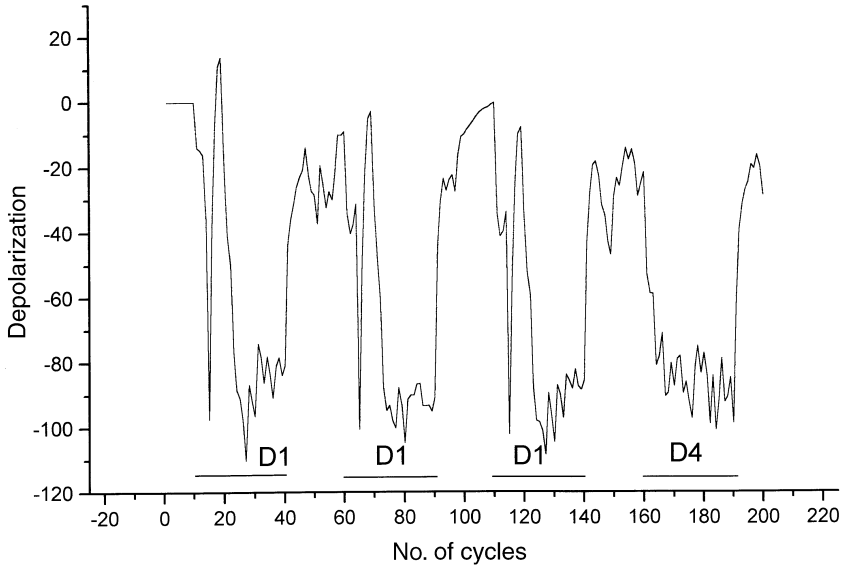


Fig. 12. Three subsequent presentations of D1 triangle for 30 cycles each and afterwards triangle D4 as “novelty” (Field potentials)

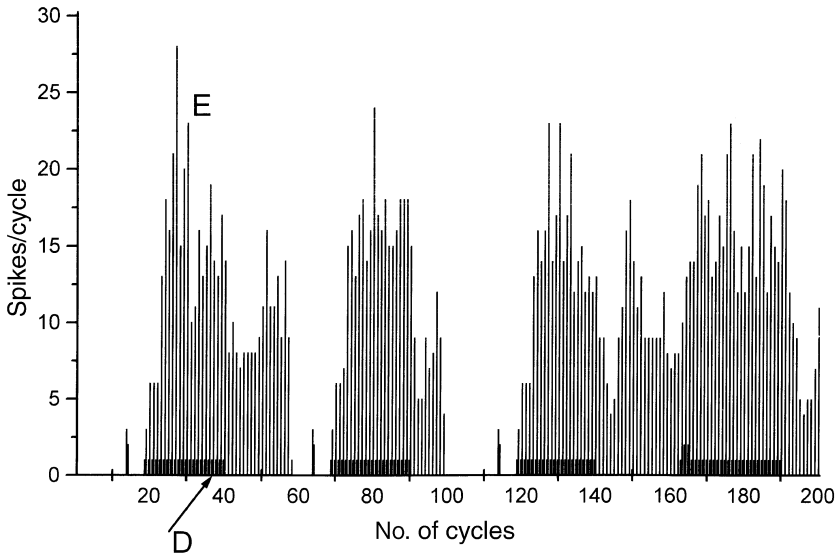


Fig. 13. Spike discharges in layer D (small dark columns) and layer E (high light columns) in the same model procedure illustrated in Fig. 12. It seems obviously that persistent activity of the cognitive neurons ensues only after decreasing of the initial irradiation (small lonely columns in layer D) and selection of the competent neurons (densely packed firing)

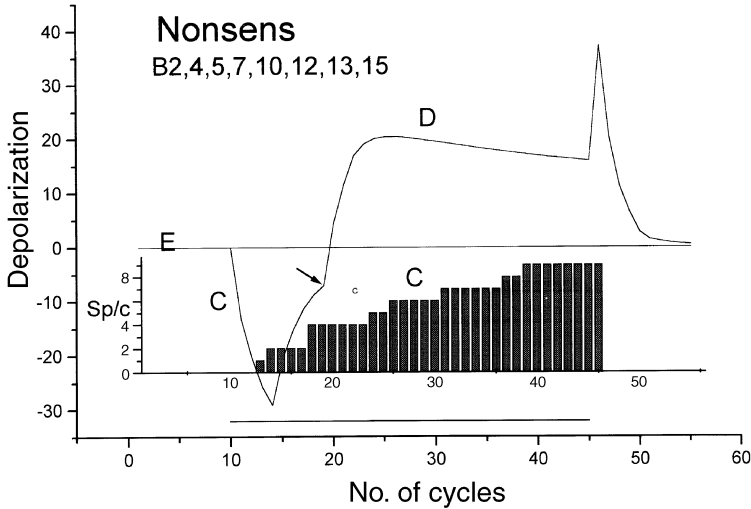


Fig. 14. Field potential and cellular firing recorded after presentation of an unknown, chessboard-like stimulus throughout 40 cycles. Two cells are firing in layer C but unable to excite firing spikes D-neurons. Compare with (primary, noncognitive) visual evoked potential illustrated in upper row of Fig. 11

the rise of E can shift to even earlier dates and P300 tends to confuse with the first positive wave (in EEG records P100). This may lead to the impression that P300 has disappeared. However, cellular records show obviously that spike discharges of E-neurons are present and begin even earlier than before. This may come from synaptic facilitations in synapses D-E. An example for a shift in E-latency is shown in Figures 12 and 13.

The field potential record of Figure D shows, that in spite of repetition of D1 triangle, P300 wave remains in essentially unchanged form proving that it is bound to cognitive content and not to “novelty”. However, at presentation of triangle D4, P300 seems to disappear, but factually it appears earlier and fuses with P100 as it can be ascertained from Figure 13, where layer D and E spike discharge patterns are illustrated throughout the experiment. Initial depolarizations of layer E are reflected in spike discharges in every case, with some delay after discharges of D, but at presentation of D4, E-spikes appear earlier after D-onset, than formerly and the fusion of P300 and P100 appears duplicated at the cellular level.

An example of non-cognitive stimulus a chessboard like pattern was applied. This was regarded as non-cognitive, because such figure was not contained and not recognized by layer D. According to this, B2, 4, 5, 7, 10, 12, 13, 15 group of thalamocortical impulses was able to evoke the picture of two lines in layer C, but only several EPSPs in layer D. Layer E was left in rest. The field potential consists therefore a surface-positive pike and a surface negative slow wave in essential analogy with the “non-cognitive” EEG signal of the experiment in upper row of Figure 11. The cellular record shows only C-spikes with rising frequency.

Relation of VERP pattern to stimulus pattern

In Figure 15 VERPs are illustrated as evoked by five different types of patterned stimuli. Number of presentation varied from 20 to 50, thus each field potential represents 20 to 50 averaged VERPs. Denotations of records refer to figurines of layer D in Figure 2.

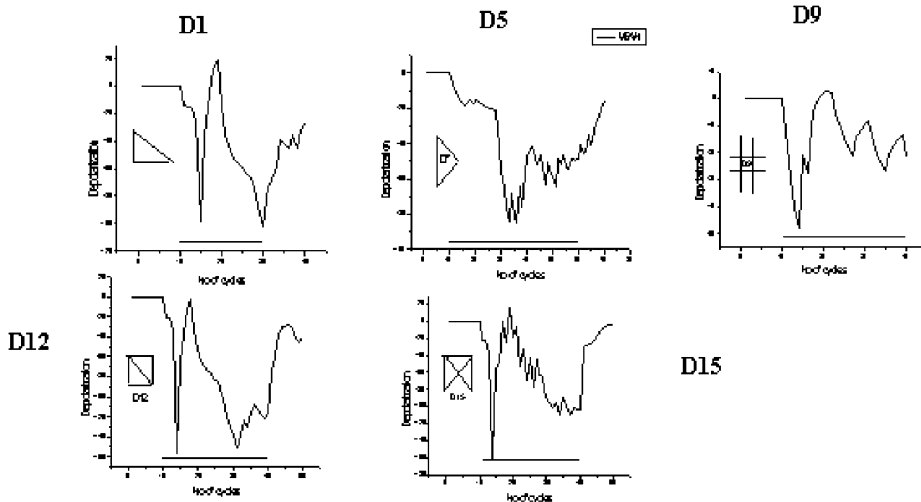


Fig. 15. Field potentials of five different types of geometrical figures recognizable by the model

The main morphological aspects can be summed up in the following points. 1. The overall structure of the model field potentials is basically the same as that of “natural” EEG records. The absence of the initial small negative wavelet and the spike-like character of the P100 wave was mentioned and explained formerly. 2. The total length, the partition of components all suggest, that one cycle of the computer simulation is in good approximation with 10 ms of the EEG records. 3. Except field potential of figurine D9 every field potential pattern contains P300. 4. Comparisons with a larger number of EEG-recorded field potentials (not illustrated here) gave a lot of parallels of inflection points being present in both samples at the same transitions between component waves. 5. Figurines consisting of fewer points required more presentations (up to 50) because summations, necessary for forwarding impulses to the next layer were built up slower. 6. Differences between field potential patterns cannot be ascribed to geometric characters of the figurines, much more to the differences in the mode of analyzing them. For example differentiation between very similar figures (e.g. small triangles) requires a more sophisticated inhibitory network than between dissimilar ones. Especially difficult task is for the system to differentiate squares from triangles, which they contain (e.g. D12 square includes triangles D1

and D4). During building-up the field potential of a more complex pattern, the cells representing their components, are transiently activated. This and the intervention of the inhibitory system influence the final complexion. The experience collected in course of modeling event related potentials has been enriched with many fine details of information processing, presumably being analogous in living systems. The study of information processing in the sensory areas may give insight also into the mechanism of retrieval, imagination and creative transformation of sensory experience.

REFERENCES

1. Callaway, E. M. (1998) Local circuits in primary visual cortex of the macaque monkey. *Ann. Rev. Neurosci.* 21, 47–74.
2. Creutzfeldt, O. D (1983) *Cortex Cerebri*. Springer Verlag, Berlin.
3. Fehér, O., Virág, T. (1996) A computer model of the visual cortex. *Neurobiol.* 4, 13–26.
4. Virág, T., Fehér, O. (1996) A computer model of processes of binocular vision in the cerebral cortex. *Neurobiol.* 4, 27–34.
5. Hebb, D. O. (1949) *The Organization of Behavior*. Wiley, Toronto
6. Hubel, D. H., Wiesel, T. N. (1968) Receptive fields and functional architecture of monkey striate cortex. *J. Physiol. (London)* 195, 215–243.
7. Hubel, D. H., Wiesel, T. N. (1972) Laminar and columnar distribution of geniculocortical fibers in the Macaque monkey. *J. Comp. Neurol.* 146, 421–450.
8. MacGregor, R. J. (1987) *Neural and Brain Modeling*. Academic Press, New York.
9. Antal, A. (1999) Event related potentials in monkey and man. PhD Thesis, Albert Szentgyörgyi Medical University, Szeged.
10. Antal, A., Alexander, E., Safarik, C., Bodis-Wollner, I. (1998) Analysis of simultaneously recorded primary and cognitive visual evoked potentials. *Clin. Neurosci.* 51, 5–11.

APPENDIX

Return to the resting membrane potential. In absence of afferent impulses the membrane potential (A) tends to return to the resting level (48 in this model) in an exponential way. From IPSP (hyperpolarization):

$$A(n + 1) = 48 + (48 - A(n)) \exp(0.69) \quad (1)$$

From EPSP (depolarization)

$$A(n + 1) = 48 + [A(n) - 48] \exp(-0.28) \quad (2)$$

where n is the number of the actual cycle.

Input to the neurons. Each neuron has 21 input ports for excitation with separate independent synaptic efficacy. Synaptic strength is dependent on the function, according to the Hebb's rule. Input to the i -th port is built up by

$$f_i(n) a_i(n) \quad (3)$$

where f_i is synaptic efficacy, and a_i one of the synaptic ports bearing it.

$$\begin{aligned} &\text{If } a_i = 1, \text{ active} \\ &0 \text{ otherwise} \end{aligned}$$

The sum of inputs arriving at the ports is

$$\Sigma f_i(n) a_i(n) \quad (4)$$

The maximal excitatory state in the n -th cycle is

$$A(n-1) + \Sigma f_i(n) a_i(n) \quad (5)$$

In which $i = 1$ to 20. If the neuron reaches the threshold, $A(n) > K$, it fires spikes (from 1 to 9) in proportion of $A-K$. This is recorded in the spike number variable S .

Change of synaptic efficacy. In neurons, when firing, the synapses are strengthened while in the rest they are weakening. An immediate measure of synaptic strength is

$$T_i(n) = t_i(n) a_i(n) 0.05 - t_i(n-1) 0.005 \quad (6)$$

The initial value of $t_i(n)$ is 0.08. Thus if a synapse is active, it strengthens with each impulse by 0.045, when inactive, it weakens by 0.005. With repetitive stimulation the synaptic strength t_i approaches a limit:

$$F_i(n) = F [1 - \exp(-t_i(n))]$$

Which may be at different values: 2, 3, 4, 5, or 10. Its relation to number of cycles is illustrated in the diagram.